# Proton-neutron interactions across the $N$ = 28 shell closure via $^{47}K(d,p)^{48}K$, and implications for the most neutron-rich phosphorus


**Spokespersons: W.N. Catford[1] and A. Matta[2]**

**[1]University of Surrey, Guildford, UK [2]LPC Caen, 1400 Caen, France**


## Science Case

The discovery of magic numbers in nuclei represents one of the cornerstones of nuclear physics. Exploring how the shell gaps evolve with nucleon number toward the drip-lines is a key goal in the physics of nuclei, with a microscopic understanding from nuclear forces presenting a major challenge for theory. As experiments access ever-more neutron-rich nuclei, the valence orbitals for protons and neutrons become more widely separated in energy where relevant matrix elements are either poorly defined or completely unknown.

The $N$ = 28 shell closure has attracted considerable scientific interest over the last decade as this is the first magic number that cannot be reproduced by calculations using two-body nucleon-nucleon interactions alone [1]. Recent experimental and theoretical studies indicate that the $N$ = 28 shell closure disappears below $Z$ = 20. Moving down from doubly-magic $^{48}Ca$, a progressive onset of deformation is found: $^{46}Ar$ is a moderately collective vibrator, $^{44}S$ shows prolate-spherical shape coexistence, $^{42}Si$ has oblate deformation, and the newly discovered $^{40}Mg$ is likely to be prolate [2]. This smooth but continuous change of nuclear shapes at $N$ = 28 is quite unique in the chart of nuclides. Throughout this region, proton-neutron forces act between valence nucleons in orbits which are different from the ones occupied in the valley of stability, thereby revealing new facets of the nuclear force which have yet to be tested.

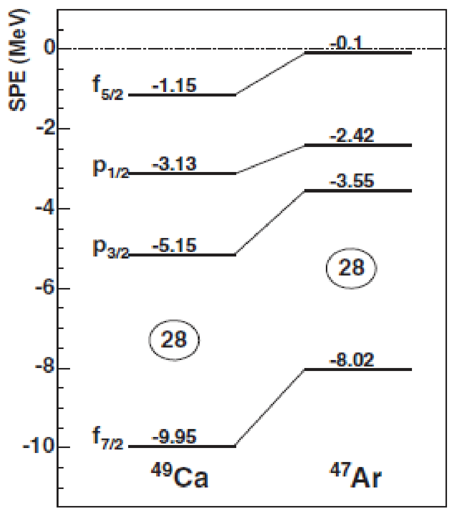


Figure 1: Single particle energies deduced from experimental data [4]. The gap at $N$ = 34 above the $p_{1/2}$ orbital appears to strengthen for elements below calcium. The interactions that cause this are still to be clearly established.

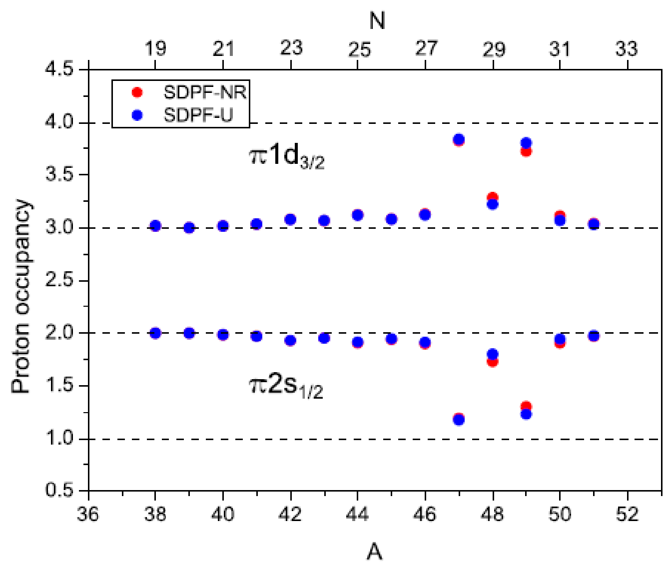


Figure 2: Theoretically calculated occupancies of the proton shell model orbitals for isotopes of potassium [5], illustrating the physics underlying the inversion of the $3/2^+$ and $1/2^+$ levels for $^{47}K$ and $^{49}K$. In these two nuclei, the ground state has a single odd proton in the $s_{1/2}$ orbital.

The neutron number $N$ = 34 has been identified as a magic number, at least in $^{54}$Ca, in a recent Letter to Nature [3]. This indicates the establishment of a significant energy gap between the $p_{1/2}$ and $f_{5/2}$ orbitals for the proton deficient $N$ = 34 nuclei. These orbital energies, and their evolution when protons are removed from below $Z$ = 20, have been studied by Gaudefroy *et al.* [4]. As shown in Fig. 1, the $N$=34 gap appears to be reinforced as protons are removed from the closed $Z$ = 20 proton shell. There have been speculations about the mechanism for this [4] but the situation is not resolved and some aspects are specific to the proton core in argon. A useful clarification is to measure the interaction between an odd proton below $Z$ = 20 with an odd neutron in the orbitals above $N$ = 28 that define the magicity of $N$=34. In the case of the $\pi(0d_{3/2})$ orbital, the interactions have been measured via the $^{39}$K($d$,$p$) and $^{37}$Cl($d$,$p$) reactions [6] and we now propose the first study to address the more exotic $\pi(1s_{1/2})$ interactions. This will be especially critical when the spectroscopy of N=29 nuclei in the region of $^{44}$P is reached experimentally.

In this proposal we focus upon the nuclear structure of the odd-odd nucleus $^{48}$K, studied via the $^{47}$K($d$,$p$) transfer reaction in inverse kinematics. Extraordinarily, this projectile has a single proton in the $\pi(1s_{1/2})$ orbital and complete $\pi(0d_{3/2})$ and $\nu(0f_{7/2})$ orbitals; this odd-$\pi(1s_{1/2})$ structure makes it an exceptionally useful projectile to study spectroscopy.

The low-lying levels of $^{48}$K (N=29) have been the subject of great interest recently at both Gammasphere and PRISMA/CLARA, due to the unique insights they offer into the cross-shell proton-neutron interaction at $N$ = 28 [7]. A particularly important subset of these levels, that we highlight here, are those arising from the interaction of an odd $1s_{1/2}$ proton with neutrons in the $0f_{7/2}$, $1p_{3/2}$, $1p_{1/2}$ and $0f_{5/2}$ orbitals (see Figure 3). These are the interactions that figure prominently in the structure of neutron-rich isotopes of phosphorus (Z = 15) all the way out to the three heaviest isotopes so far observed [8], $^{44,45,46}$P (N = 29, 30, 31).

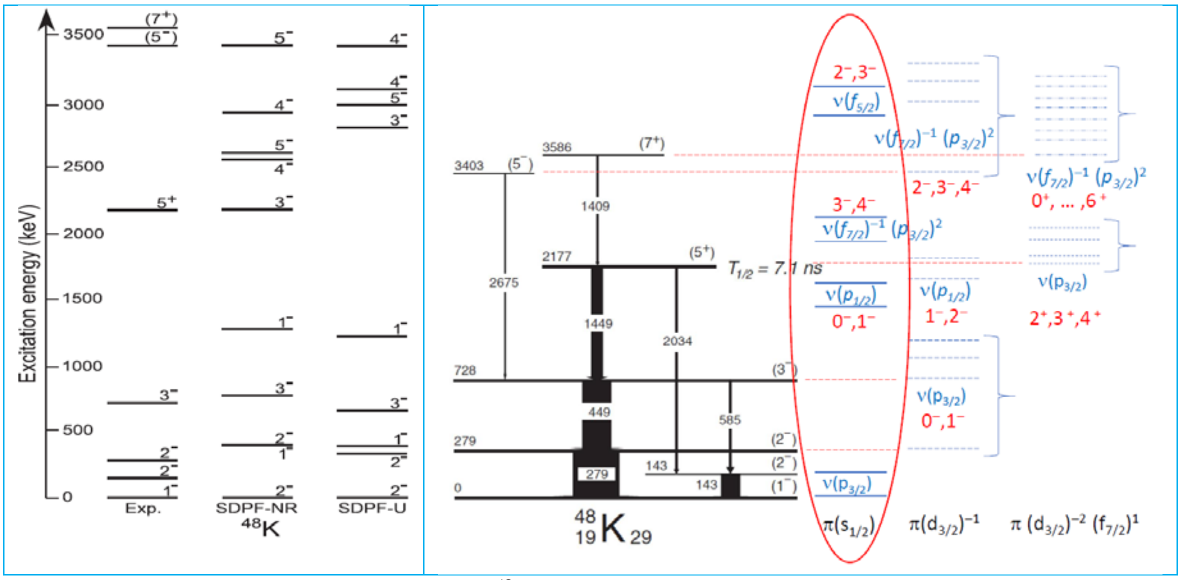


Figure 3: (left) experimental level scheme for $^{48}$K [7], compared to two recent shell model calculations [7]; (right) the observed levels [7] compared with the simple shell model configurations expected to occur in $^{48}$K. The positive parity states expected from the collective octupole excitation of the core are not shown. The ellipse identifies the states populated in (d,p) by transfer into the (mostly empty) $p_{3/2}$, $p_{1/2}$ and $f_{5/2}$ orbitals and the (mostly occupied) $f_{7/2}$ orbital, and this effectively predicts the spectrum of $^{44}$P. ($S_n$=4.644 MeV for $^{48}$K.)

The reaction $^{47}$K($d$,$p$)$^{48}$K is highly selective towards the states in $^{48}$K that are determined by the $\pi(1s_{1/2}) \otimes \nu(fp)$ interactions. This is because, as noted above, the ground state of $^{47}$K has $J^{\pi} = 1/2^+$ rather than the more obviously expected $3/2^+$. This, in turn, is due to the effects of the closed $\nu(0f_{7/2})$

subshell on the energies of the proton orbitals and was confirmed recently in magnetic moment measurements at ISOLDE [5]: the usual $\pi(0d_{3/2})^{-1}$ configuration for potassium isotopes is replaced in the $^{47}$K ground state by the $\pi(1s_{1/2})(0d_{3/2})^4$ configuration. The more obvious $\pi(0d_{3/2})^{-1}$ configuration occurs at an excitation energy of 0.36 MeV [5]. Thus, whilst the low-lying levels of $^{48}$K will include the couplings of both $1s_{1/2}$ and $0d_{3/2}$ protons to *fp*-shell neutrons, the reaction $^{47}$K(*d*,*p*)$^{48}$K will select specifically the $\pi(1s_{1/2}) \otimes \nu(fp)$ states that are so relevant to the structure of N=29-31 isotopes down to $^{44-46}$P. Such states cannot be isolated by any alternative method.

The dominant configurations for the two lowest $2^-$ states in $^{48}$K (at 143 and 279 kev, see Fig.3) have been identified on the basis of the observed gamma-ray decay scheme [7], but the actual mixing can only be measured in the experiment that we propose here. The other states arising from $\pi(1s_{1/2})\otimes \nu(fp)$ configurations (included in the ellipse in Fig. 3) have not previously been observed. They will also be mixed with other states of the same spin and parity and this mixing will be quantified by measuring the spectroscopic factors via the present (d,p) study. This mixing also incidentally means that the experiment will give information on the more-weakly populated configurations that are based upon coupling with $\pi(d_{3/2})^{-1}$. In order to isolate and measure these weaker states it will be essential to have the high energy resolution for gamma-ray detection as provided by AGATA and to gate on these gamma-ray transitions. Overall, it is remarkable how little is known about the $^{48}$K level scheme, given that it differs from the stable nucleus $^{48}$Ca only by the exchange of a neutron for a proton.

The measurement of the states in $^{48}$K produced by the coupling $\pi(1s_{1/2})\otimes \nu(fp)$ is part of what will one day be a sequence of measurements including also the isotones $^{46}$Cl and $^{44}$P (see Fig.4), because the ground state of $^{45}$Cl is a similar $1/2^+$ "intruder" and also $^{43}$P should have $J^\pi=1/2^+$ for its ground state. The $^{44}$P, $^{46}$Cl and $^{48}$K will represent the coupling $\pi(1s_{1/2})\otimes \nu(fp)$ in the cases where the $\pi(d_{3/2})$ orbital contains, respectively, 0 or 2 or 4 neutrons (see Fig. 5). The experiment using a $^{45}$Cl beam will be possible using day-one FRIB beams.

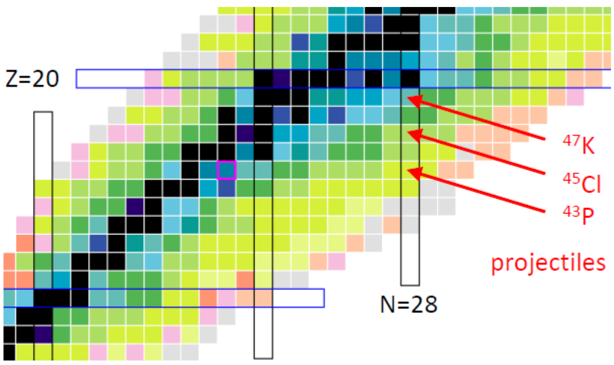


Figure 4: The N=28, odd-Z isotones that have ground states with spin and parity $1/2^+$ and which therefore give a simple and unique population of states when used as projectiles in (d,p) transfer reactions.

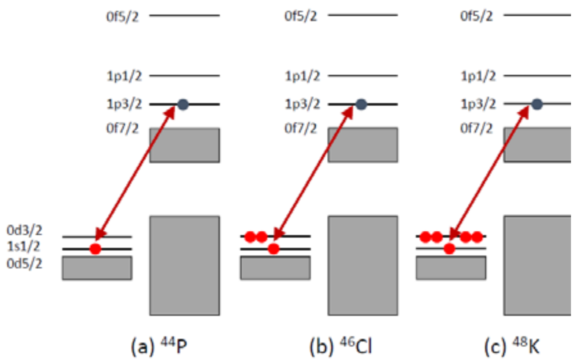


Figure 5: The N=29, odd-Z isotones for which the low-lying excited states represent the coupling of an odd $1s_{1/2}$ proton to the various fp-shell orbitals, but with different proton occupancy of the 1d3/2.

The rich nuclear structure information that this experiment will begin to expose has been identified and compared in detail with state-of-the-art shell model calculations in ref. [9]. Some relevant results are displayed in Fig.6. Whilst this shell model analysis offers many valuable insights, it is still far from a satisfying picture because it fails at the very beginning to predict the $1^-$ state as the ground state of $^{48}$K, as observed experimentally [7] (cf. Fig.3). An interesting feature of the shell model calculations is the lowering in energy of the states in which a neutron is promoted from $\nu(0f_{7/2})$ to the $\nu(1p_{3/2})$ orbital so that it joins the final neutron to form a pair, leaving a $\nu(0f_{7/2})^{-1}$ structure of 2p1h nature. The centroid energy of these states is indicated in Fig.6 by the red diamond symbols (♦). The predicted amount of mixing for this configuration into the ground state is also shown in Fig.6. This mixing, indicating a breaking of the N=28 shell, is found to arise less from the monopole shift (which does contribute) and more from the increased collectivity induced by the quasi-degeneracy of the $\pi(0d_{3/2})$ and $\pi(1s_{1/2})$ orbitals ($\Delta\ell$=2). However, these shell model interpretations need to be verified experimentally.

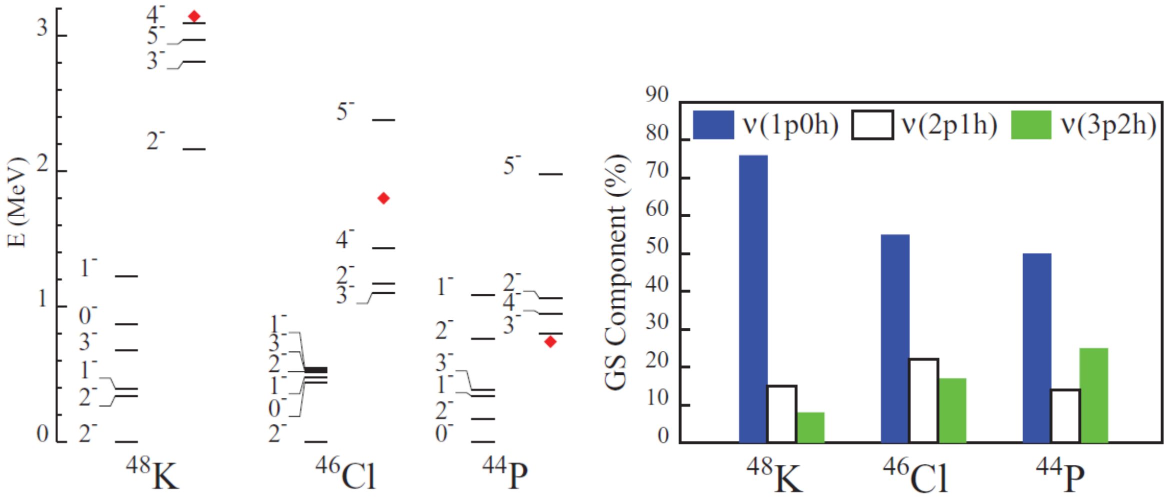


Figure 6: Shell model calculations of the evolution of structure in N=29 isotones using the SPDF-U interaction [9]. The $^{48}$K level scheme also appears in Fig.3, where it is seen to fail at reproducing the 1$^{-}$ state as the ground state. The reduction of the N=28 gap, arising from increased proton collectivity, is discussed in the text. The consequent mixing into the ground state of configurations that break the N=28 closure is shown on the right.

## Experimental Details

The experiment is planned to use the MUGAST + VAMOS + AGATA set-up. The arrangement of silicon detectors around the target in the Géant4 simulation is shown in Figure 7. A solid target of deuterated polythene $CD_2$ of thickness 0.5 mg/cm$^2$ will be used, to maintain reasonable energy resolution for $^{48}$K final states. The MUGAST array will measure protons from (d,p) over an angular range of 105° to 170° in the laboratory and elastically scattered deuterons just forward of 90°. The elastic scattering will allow the extraction of absolute cross sections as in our previous (d,p) work at VAMOS [10-12].

The beam will be $^{47}$K at the maximum energy of 7.7 MeV/nucleon and the optimum charge state of 8$^{+}$. A possible contaminant is $^{47}$Ca at up to the 10% level. VAMOS (at 0°) is required to remove reactions occurring on the carbon in the $CD_2$ target and will be operated at rates up to $10^5$ pps. The different charge states of the stripped beam will be separated by 12 cm at the focal plane of VAMOS (assuming 1.8 cm/% dispersion) and we anticipate recording the strongest two charge states. Calculations suggest the dominant state will be q=(Z-1) with 70% of the yield. The (d,p) reaction products will arrive between 0.6 cm and 2.0 cm higher in rigidity than the beam (for excitation energies from 0 to 4 MeV and proton angles from 105° to 170°) and the elastic scattering will arrive at up to 3 cm lower in rigidity. This setup mirrors our experiments using beams of $^{20}$O [11] and $^{26}$Ne [12] at VAMOS, where the direct beam was not intercepted. If more intensity is potentially available we will investigate intercepting the beam at the focal plane using narrow stoppers, as was done in our experiment using $^{24}$Ne [10]. VAMOS also provides a means to reject reactions due to any $^{47}$Ca beam contaminant, using both the 8% difference in dE/dx and also the stripping to a charge state one higher.

AGATA will be used to record coincident gamma-rays (all states in $^{48}$K are bound up to 4.64 MeV) and correct for the Doppler shift from the fast moving ($\beta$=0.13) ejectiles. The energy resolution is essential to identify the individual states in the odd-odd nucleus $^{48}$K. Inspection of Fig.3 indicates that gamma-decays to the ground state or low-lying first excited state can be expected for the most strongly populated states in the (d,p) transfer, AGATA's good efficiency and Doppler correction up to 4 MeV will be important.

AGATA is also vital because the gamma-ray decay scheme will be the key observation to distinguish between the states of spin $j=\ell+1/2$ and $j=\ell-1/2$ populated using the spin 1/2 projectile, where the differential cross section for the transfer provides the $\ell$ value.

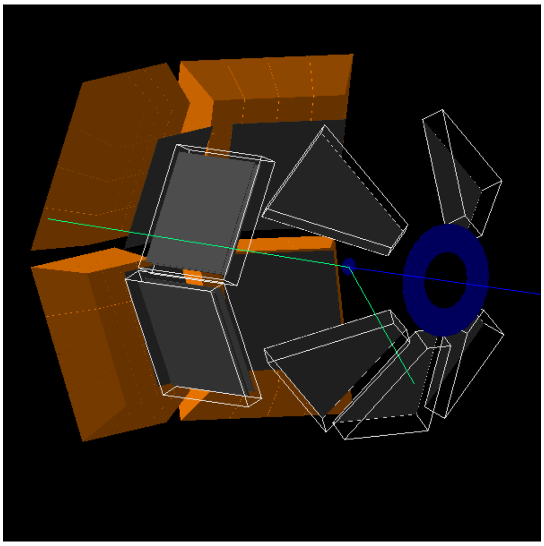

Figure 7: The MUGAST setup showing the beam entering from the right, with the GASPARD trapezoid detectors for (d,p), the TRACE squares and the MUST telescopes at forward angles. Diagram from Géant4.

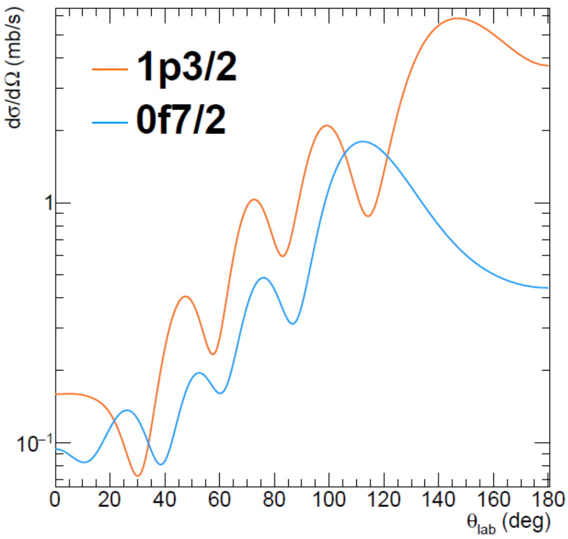


Figure 8: Shown in the laboratory frame, the ADWA predicted differential cross sections for p- and f-wave transfer on $^{47}K$ to states in $^{48}K$ and $C^2S=1$. The experiment will study angles 105° to 170° in detail.

## Beam Time Request

To estimate the beam time requirement for the present proposal, we performed ADWA calculations of the differential cross section using the code TWOFNR [13], see Figure 8. We performed Géant4 simulations to estimate the energy resolution that can be achieved from the proton energies/angles alone. The predicted kinematic data assuming a 0.5 mg/cm$^2$ $CD_2$ target are shown in Figure 9 and in Figure 10 the same results are shown as an excitation energy plot deduced from the protons populating the ground state and 4 MeV level. Given that, for example, four states will be populated below 1 MeV it is clear that any thicker target should be avoided and that the resolution provided by AGATA will be of paramount importance. We plan to use gamma-ray energy gating to extract differential cross sections for individual states as we did in our previous study of $^{26}Na$ [14].

Assuming a $^{47}K$ beam intensity of 1 x $10^5$ pps and a $CD_2$ target of 0.5 mg/cm$^2$, Table 1 gives the expected yields in 15UT for a spectroscopic factor of unity. This may be a reasonable estimate for the transfers to $\nu(1p_{3/2})$, $\nu(1p_{1/2})$ and $\nu(0f_{5/2})$ but the $\nu(0f_{7/2})$ transfer is blocked and will be much smaller. We aim to measure angular distributions for resulting protons from the $^{47}K(d,p)^{48}K$ transfer, using at up to 10 angular bins between 170° and 105° degrees in the laboratory frame. Such coverage will allow for the accurate determination of the expected strong $l$ = 1 and 3 components of key states in $^{48}K$ using gamma-ray gated data. A further 6UT will be required for beam tuning and setting up.

<u>Beamtime requirement</u>:

15UT (data acquisition), plus 6UT (beam optimisation and setting up) = **<u>21 UT TOTAL</u>**

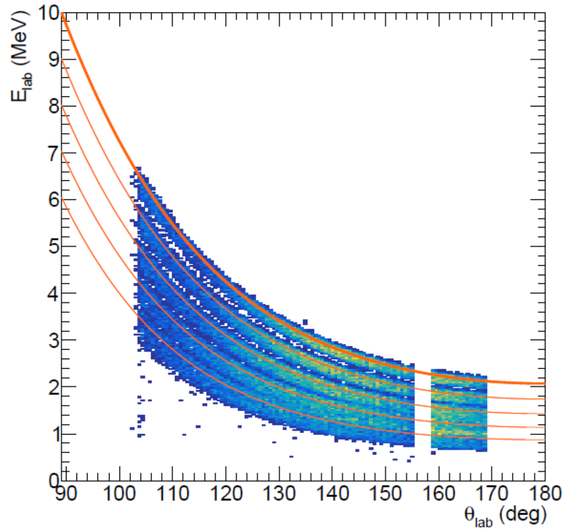


Figure 9: Simulated results for the proton energy as a function of laboratory angle for (d,p) assuming states in $^{48}$K at 0 MeV (upper locus) plus 1,2,3 and 4 MeV.

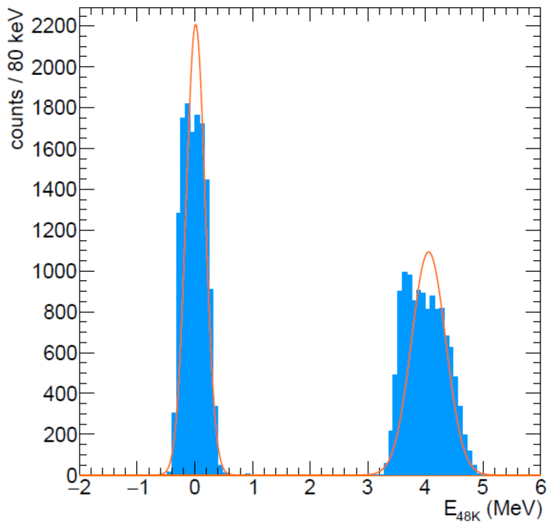


Figure 10: Results of the simulations in Fig.9 plotted in terms of the deduced excitation energy in $^{48}$K, for the ground state and the supposed state at 4 MeV.

| E | FWHM (keV) | orbital | J | $\sigma$ (mb) | $N_R$ | $N_D$ | $N_\gamma$ | $Eff_\gamma$ (%) |
|---|---|---|---|---|---|---|---|---|
| g.s | 600 | 1p3/2 | 2 | 21 | 34k | 13k | - | - |
| 1 | 680 | 1p3/2 | 2 | 24 | 39k | 14k | 980 | 7 |
| 2 | 800 | 1p3/2 | 2 | 26 | 43k | 15k | 750 | 5 |
| 3 | 960 | 1p3/2 | 2 | 26 | 43k | 15k | 600 | 4 |
| 4 | 1080 | 1p3/2 | 2 | 23 | 38k | 12k | 360 | 3 |
| g.s | 600 | 0f7/2 | 4 | 8 | 13k | 5k | - | - |
| 1 | 680 | 0f7/2 | 4 | 10 | 17k | 6k | 420 | 7 |
| 2 | 720 | 0f7/2 | 4 | 14 | 23k | 7k | 350 | 5 |
| 3 | 840 | 0f7/2 | 4 | 18 | 29k | 9k | 360 | 4 |
| 4 | 960 | 0f7/2 | 4 | 24 | 39k | 12k | 360 | 3 |

Table 1: Assuming spectroscopic factor $C^2S=1$, the yields in the columns $N_D$ and $N\gamma$ represent the expected numbers recorded over 15UT of beam for protons from (d,p) and coincident ground-state gamma-rays respectively. A $^{47}$K beam intensity of $10^5$ pps was assumed.

## References


[1] J.D. Holt *et al.*, Journal of Physics G 39, 085111 (2012)
[2] T. Baumann *et al.*, Nature 449, 1022 (2007)
[3] D. Steppenbeck *et al.*, Nature 502, 207 (2013)
[4] L. Gaudefroy *et al.*, Phys. Rev. Lett. 97, 092501 (2006)
[5] J. Papuga *et al.*, Phys. Rev. C 90, 034321 (2014)
[6] C.L. Fink and J.P. Schiffer, Nucl. Phys. A225, 93 (1974)
[7] W. Krolas *et al.*, Phys. Rev. C 84, 064301 (2011)
[8] M. Thoennessen, Atomic Data and Nucl. Data Tables 98, 933 (2012)
[9] L. Gaudefroy, Phys. Rev. C 81, 064329 (2010)
[10] W.N. Catford *et al.*, Phys. Rev. Lett. 104, 192501 (2010)
[11] B. Fernandez-Dominguez *et al.*, Phys. Rev. 84, 011301 (R), (2011)
[12] S.M. Brown *et al.*, Phys. Rev. C 85, 011302 (2012)
[13] J. A. Tostevin, University of Surrey version of the code TWOFNR (of M. Toyama, M. Igarashi and N. Kishida) and code FRONT (private communication); available at http://www.nucleartheory.net/NPG/code.htm
[14] G.L. Wilson *et al.*, Phys. Lett. B 759, 417 (2016)